

NANO EXPRESS

Open Access

Bi-stable resistive switching characteristics in Ti-doped ZnO thin films

Adnan Younis, Dewei Chu* and Sean Li

Abstract

Ti-doped ZnO (ZnO/Ti) thin films were grown on indium tin oxide substrates by a facile electrodeposition route. The morphology, crystal structure and resistive switching properties were examined, respectively. The morphology reveals that grains are composed of small crystals. The (002) preferential growth along *c*-axis of ZnO/Ti could be observed from structural analysis. The XPS study shows the presence of oxygen vacancies in the prepared films. Typical bipolar and reversible resistance switching effects were observed. High R_{OFF}/R_{ON} ratios (approximately 14) and low operation voltages within 100 switching cycles are obtained. The filament theory and the interface effect are suggested to be responsible for the resistive switching phenomenon.

Keywords: Electrodeposition, Nanostructure, Resistive switching

Background

Resistance switching in metal oxide structures has attracted considerable attention because of its potential application to non-volatile memories [1-5]. Resistive random access memories (RRAMs) have many advantages over other technologies of data storage, such as much faster reading and writing rate, smaller bit cell size and lower operating voltages and very high retention time up to 10 years [2,6-8].

In general, the metal oxide thin films are prepared by physical methods, such as radio frequency magnetron sputtering and pulsed laser deposition, etc. It not only involves high fabrication cost but also limit the size and massive production. On the other hand, chemical methodologies, such as chemical bath deposition and hydrothermal, suffer from the problems of low crystallinity, disconnection of substrate and film or high-temperature calcinations. Compared with the aforementioned techniques, electrodeposition provides an effective way to fabricate high-quality metal oxide thin films at low temperature and ambient atmosphere. Moreover, in this process, the deposition of metal oxide layers on the substrate is driven by the external electric field. Therefore, it is facile to precisely control the layer microstructure

by this method and further design heterostructures with novel functionalities.

To date, various methods including doping [9], interface engineering [10] and nanoparticle incorporation [11,12] were used to improve the performance of RRAM devices. The effects of Au and Pt nanoparticles embedded in ZrO_2 and TiO_2 oxide films have also been studied [12,13].

Among the resistance switching materials, ZnO is especially attractive for its several unique advantages, such as the coexistence of unipolar and bipolar switching behaviour [14,15], the larger high resistance state to low resistance state (HRS/LRS) window [16] and the transparent and flexible application aspects [6,17]. The doping method has already been adopted to optimize the switching performance of ZnO, including Mn, Co, Cu and Ga [15,16,18-20], but the switching properties were not as optimized as for practical applications. Very few studies of the electric conduction mechanism for Ti-doped ZnO films have been reported [21-23]. Since the ionic radius of titanium is smaller than that of the zinc, when titanium atoms doped into a ZnO lattice, they act as scattering centres/donors by providing two free electrons. However, only a small amount of doped Ti^{4+} could induce more electrons and avoid acting scattering centres [24]. Also, Ti-doped ZnO films have more than one charge valence state in comparison to that of the ZnO films doped with other Group III elements.

* Correspondence: d.chu@unsw.edu.au
School of Materials Science and Engineering, University of New South Wales, Sydney, NSW 2052, Australia

The Ti precursor in aqueous solution controls the hydrolysis process of Ti ions, and this reaction is very fast in conventional precursors, such as TiCl_4 . The coordination number of Ti is six; therefore, ammonium hexafluorotitanate is more stable, and thus, it is suitable to use as a dopant. In this present work, we find that ammonium hexafluorotitanate is the most suitable compound for Ti doping and for controlled structural morphology.

In this paper, a study has been carried out on resistance switching properties of Ti-doped ZnO, where the films were prepared by a simple electrochemical deposition method at low temperature. Ti dopants were introduced into ZnO in order to enlarge the memory window via increasing the resistivity of the high-resistance state.

Methods

Electrodeposition was carried out using an Autolab 302 N electrochemical workstation (Metrohm, Utrecht, The Netherlands). A standard three-electrode setup in an undivided cell was used. ITO (indium tin oxide) (9.3 to 9.7Ω , $1.1 \text{ mm} \times 26 \text{ mm} \times 30 \text{ mm}$, Asahi Glass Corporation, Japan) was used as the working electrode while platinum foil ($0.2 \text{ mm} \times 10 \text{ mm} \times 20 \text{ mm}$) as the counter electrode. The distance between the two electrodes was 30 mm . The reference electrode was an Ag/AgCl electrode in a 4-M KCl solution, against which all the potentials reported herein were measured.

The ITO substrates were first cleaned by detergent, then rinsed well with ethanol and DI water and then electrodeposited in a solution of 0.1 M $\text{Zn}(\text{NO}_3)_2 \cdot 6\text{H}_2\text{O}$ with 2% $(\text{NH}_4)_2\text{TiF}_6$ at 1 mA for 30 min , at 75°C . The phase composition of the samples was characterized by X-ray powder diffraction (Philips X'pert Multipurpose X-ray Diffraction System with $\text{Cu K}\alpha$; Philips, Amsterdam, The Netherlands). The morphologies of the samples were observed by scanning electron microscopy (Nova Nano SEM 230, FEI, Hillsboro, OR, USA). To measure the electrical property of the films, Au top electrodes were patterned and deposited by sputtering using a metal shadow mask. Voltage–current curves of the films were measured using an Autolab 302 N electrochemical workstation controlled with Nova software (with a possible error in current and voltage values as $\pm 5\%$; Nova Software, Chongqing, China). All measurements were repeated at least twice to confirm the results. During measurement, the working electrode and sensor electrode were connected to the top Au electrode, and the reference and counter electrode were connected to the ITO substrate.

X-ray photoelectron spectroscopy (XPS) was performed with an ESCALAB250Xi spectrometer (Thermo Fisher Scientific, Waltham, MA, USA) using a monochromatized Al K alpha X-ray source ($h\nu$) 1486.6 eV with 20 eV pass

energy. Hall effect measurements were carried out by the Accent HL5500PC (Nanometrics, Milpitas, CA, USA). All measurements were performed at room temperature.

Results and discussion

The electrochemical synthesis of ZnO is a four-step process: First, nitrate ions and H_2O are electrochemically reduced at the surface of the working electrode, resulting in an increase in the local pH value in the vicinity of the electrode (Equations 1 and 2). Then, the increase in the local pH leads to the precipitation of zinc ions as zinc hydroxide ($\text{Zn}(\text{OH})_2$, Equation 3) at a suitable temperature, and $\text{Zn}(\text{OH})_2$ can be transformed into ZnO. In the presence of Ti^{4+} , part of the Ti^{4+} ions can be incorporated into ZnO lattices.

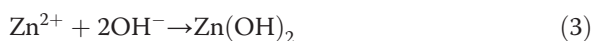
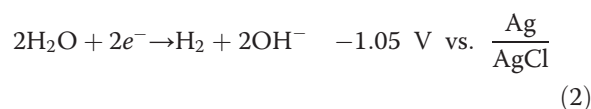
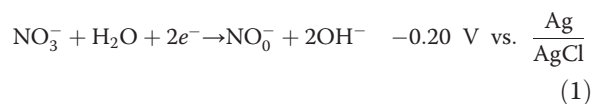


Figure 1a shows the SEM images of Ti-ZnO film. It is apparent that the grains are formed by many small crystallites aggregated with irregular shapes. In the inset of the same figure, a cross-sectional image was presented which shows film thickness as approximately 330 nm . EDS elemental maps are shown in Figure 1b,c,d. The O, Zn and Ti elemental maps have the same spatial distribution. This indicates a quite uniform distribution of elements in the synthesized products and demonstrates that the ZnO films are homogeneously doped with Ti. The EDS spectra and element atomic percentage compositions were presented in the supporting information in Additional file 1: Figure S1.

The XRD pattern of the Ti-doped ZnO film (inset pure ZnO film) was displayed in Figure 2. The XRD patterns of the films are consistent with the hexagonal lattice structure, and a strong (002) preferential orientation is observed. It implies that the Ti atoms may substitute the zinc sites substitutionally or incorporate interstitially in the lattice. From Figure 2, it can be found that the locations of the diffraction peaks slightly shift towards higher diffraction angles, which illustrate the change in interplanar spacing (d -value). This is because of the different ionic radii between Ti^{4+} (0.0605 nm) and Zn^{2+} (0.74 nm); it is within the expectation that the

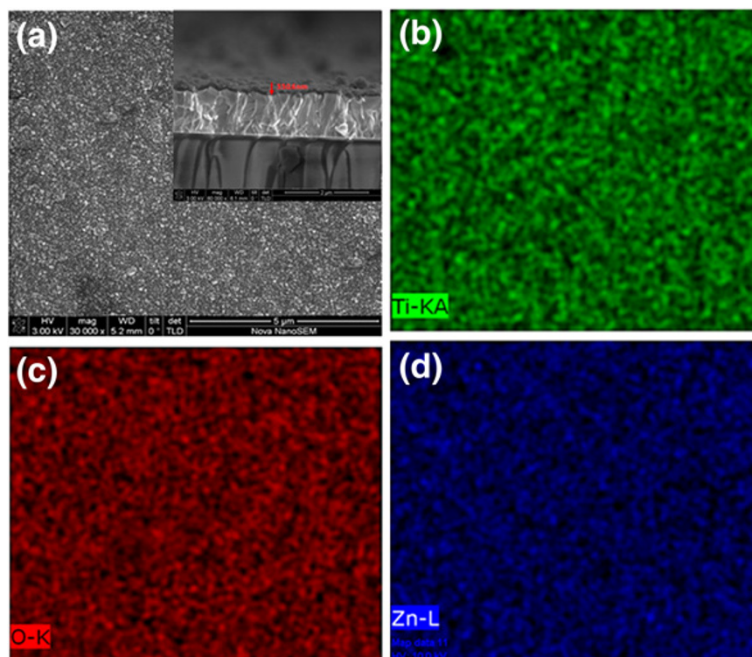


Figure 1 The surface morphology of Ti-ZnO film. (a) The SEM (inset cross-sectional image) and EDS mapping (b, c and d) images of Ti-ZnO films.

diffraction peak position shifts, indicating that Ti^{4+} substitutes Zn^{2+} position in ZnO lattices.

The typical I-V characteristics of RRAM cell based on the Au/2% Ti-ZnO/ITO was carried out by sweeping voltage and at a speed of 0.01 V/s, in the sequence of $0 \rightarrow 3 \rightarrow 0 \rightarrow -3 \rightarrow 0$ V as shown in Figure 3a. During the measurements, the bias voltages were applied on the TE with BE grounded, and neither a forming process nor a current compliance was necessary for activating the memory effort. For the Ti-doped ZnO sample, with the

increase of positive voltage, a significant change of resistance from the HRS to the LRS was observed at about 2.9 V, which is called the ‘set’ process. Subsequently, an opposite ‘reset’ process could also be seen when sweeping the voltage reversely to negative values, as evidenced by a two-step switching from LRS to HRS (Figure 4a). The first switching occurs at approximately -2.3 V (with I_{RESET} as 5.7 mA), and the second switching takes place at approximately -2.7 V (with I_{RESET} as 0.17 mA), after the resistance of the cell stays in an intermediate state for a short while. The multistage reset process observed in our sample might be due to the ruptures of multifilaments with different threshold potentials (V_{th}). This phenomenon also gives rise to the concept of multilevel data storage as long as an effective control for V_{th} could be realized. The resistive switching behaviour of our sample exhibits a typical bipolar nature, that is, the sample device can only be written with a positive bias and erased with a negative one, as this happened in our sample device during numerous measurements.

For more understanding of the conduction and switching mechanisms of the memory device, the I-V characteristics are replotted in a log-log scale. Figure 3b shows the logarithmic plot of the previous I-V curve for the positive voltage sweep region, while it is similar for the negative branch. The I-V curve in LRS clearly shows an ohmic behaviour, which might be due to the formation of conductive filaments in the device during the set process. However, the conduction mechanism in off

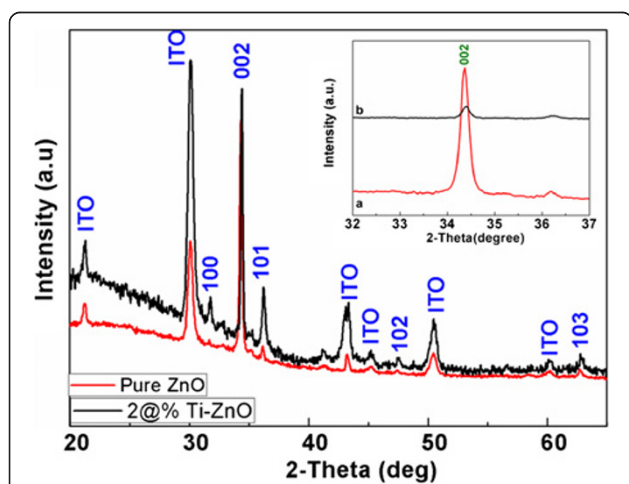
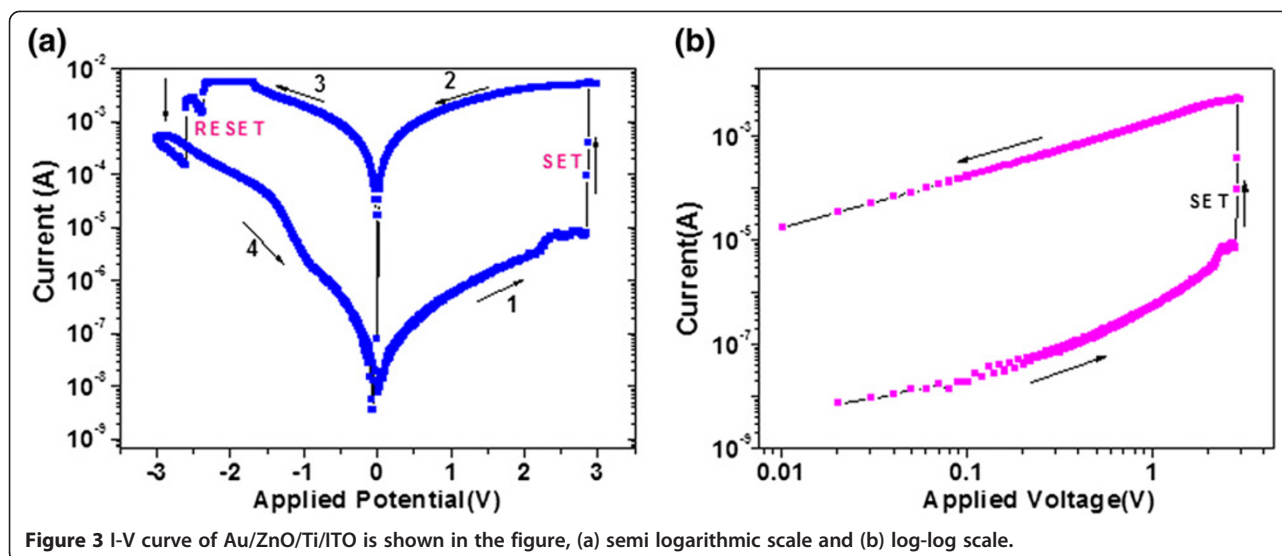


Figure 2 X-ray diffraction patterns of pure and 2% Ti-doped ZnO film (inset, magnified (002) peak).

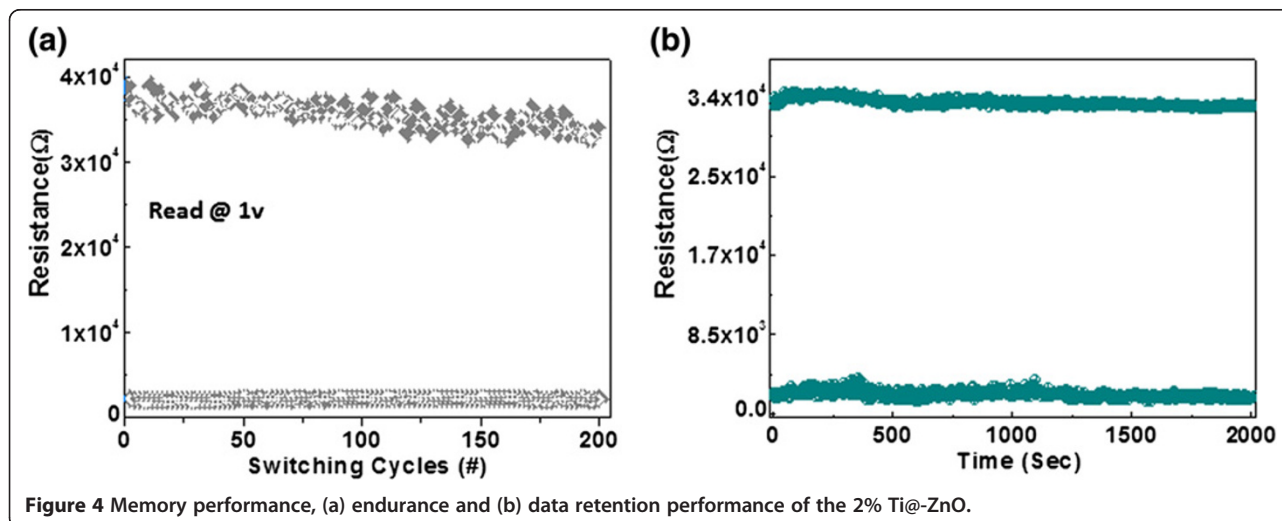


state is much more complicated. The charge transportation in this region is in agreement to the classical trap-controlled space-charge-limited conduction (SCLC), which consists of three regions: the ohmic region ($I \propto V$), the Child's law region ($I \propto V^2$) and the steep current increase region [25]. The totally different conduction behaviours in these two states (LRS and HRS) also suggest that the high conductivity in on-state device should be a confined, filamentary effect rather than a homogeneously distributed one. This indicates the fact that the active medium is much smaller than the device size, providing a potential of scaling.

The endurance characteristics of the Au/ZnO: Ti/ITO memory cell are shown in Figure 4a. The memory window defined by the two resistance states, i.e., $(R_{OFF} - R_{ON}) / R_{ON} \approx R_{OFF}/R_{ON}$, is more than 14. This is a high memory margin, making the device circuit very easy to distinguish

the storage information between '1' and '0'. The resistance of the HRS scatter in a certain extent during cycling. However, due to high R_{OFF}/R_{ON} ratio of the present device, this kind of scattering may be tolerated. It can be seen that the memory margin keeps beyond 14 times during cycling, and the cell shows little degradation after 100 repeated sweep cycles. The endurance measurements ensured that the switching between on and off states is highly controllable, reversible and reproducible. After the device was switched on or off, no electrical power was needed to maintain the resistance within the given state.

To further demonstrate the stability of the resistive switching properties, data retention was gauged by examining the current level of the device in the on state over a long period of time (>2000 s) in air ambient. In this case, no appreciable change in resistance ratio (HRS/LRS) was observed in these devices, as shown in Figure 4b, while



the information storage in these devices is likely to persist for an even longer time judging from the present trend of data.

The current–voltage measurements of pure ZnO sample were also performed and presented in the supporting information in Additional file 1: Figure S2. The memory margin of the device with 2% Ti@-ZnO was much better than the standard device (pure ZnO) as shown in Additional file 1: Figure S3. We also did perform the same measurements for both devices (pure and 2% Ti@-ZnO) without gold top electrode to see the possible effect of top electrode (results not shown here). Interestingly, both devices exhibited almost the same results as with the gold top electrode suggesting that gold top electrode is not playing critical/dominating role in resistive switching characteristics of these devices.

The XPS measurements were carried out to investigate the surface chemical compositions and bonding states of the as-prepared sample. XPS analysis done on this sample shows the presence of Ti along with Zn and O. The binding energies of Ti $2p_{3/2}$ and $2p_{1/2}$ in ZnO/Ti are approximately 458.3 and approximately 464.1 eV, in agreement with the reported tetrahedral (Ti^{4+}), as shown in Figure 5a [26]. Hence, tetravalent Ti may be replacing two divalent Zn atoms in ZnO forming a solid solution of 2% Ti-doped ZnO. Three peaks at 529.8, 531.3 and 532.7 eV can be observed in O 1s XPS spectra (Figure 5b). The peak at 529.8 may be the character spectra of oxygen in ZnO structure [27]. The little oxygen peak at 531.3 eV can be assigned to the oxygen in TiO_2 [28], whilst the O peak at 532.7 may be attributed to chemisorbed oxygen ions present in the sample [26]. The chemisorbed oxygen impurities could be O^{2-} , O^- , O_2^- , O_2^{2-} and OH^- ions as well [29,30], so the binding energy not only depends on the charge of oxygen

species but also depends upon the crystallographic orientation of the bounded surface to which the oxygen atoms or molecules are bound [29], which points to the nonstoichiometric nature and presence of oxygen vacancies present in the film. Also, our synthesis method is a solution-based method, so these oxygen vacancies can easily be generated during growth process. From previous reports, it was believed that electrochemical migration of oxygen vacancies is the dominating factor in the resistive switching behaviour [31,32]. So we can also expect that the oxygen-deficient nature of the film which contains oxygen vacancies initially will enhance the resistance switching nature of prepared 2% Ti@-ZnO film.

In our recent study [33], the resistive switching characteristics of pure ZnO were improved (on/off, approximately 7) with Co doping in ZnO. In the present report, with the addition of Ti in ZnO, the resistive switching characteristics were further improved with on/off ratio (>14) and data retention time of 2,000 seconds was achieved.

Conclusions

Ti-doped ZnO thin films were prepared by a facile electrochemical deposition method. The SEM, XPS and EDS mapping indicates that Ti is homogeneously doped in ZnO films. The Ti-doped ZnO film had a similar structure to that of the pure ZnO film and had a preferential orientation in the (002) direction. The prepared film exhibits excellent resistance switching behaviour with a HRS/LRS ratio of about 14 during endurance test, much better than pure ZnO. In addition, the dominant conduction mechanism of LRS and HRS were explained by trap-controlled space-charge-limited conduction. The present work demonstrates that Ti doping can further enhance switching

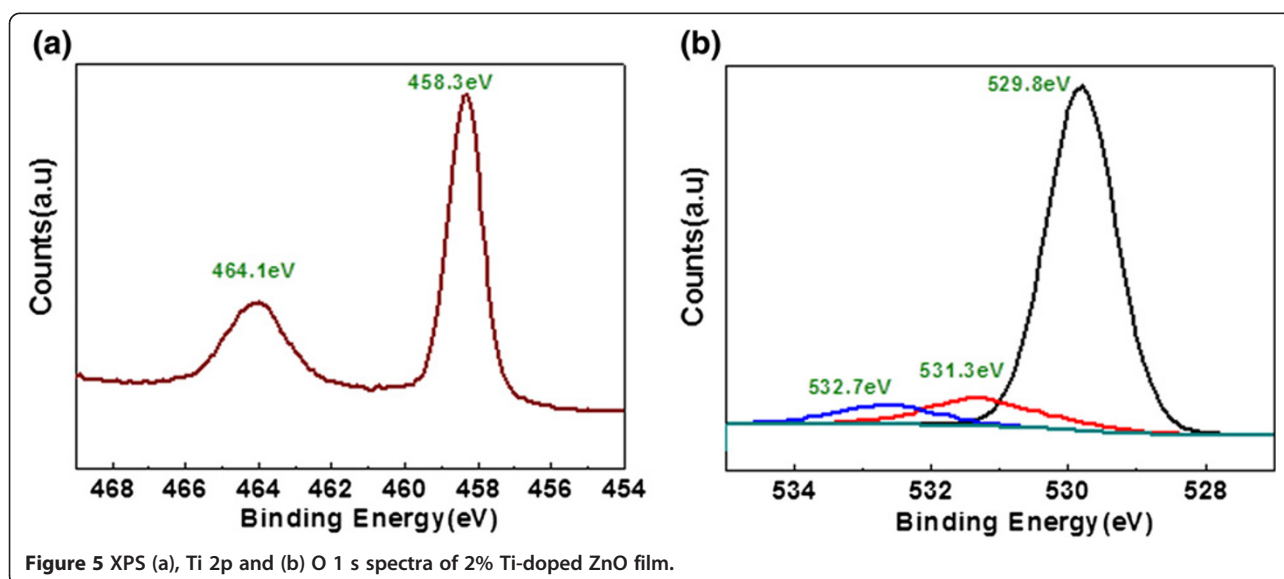


Figure 5 XPS (a), Ti 2p and (b) O 1s spectra of 2% Ti-doped ZnO film.

characteristics of pure ZnO films and thus have the potential for next-generation non-volatile memory applications.

Additional file

Additional file 1: Figures S1 to S3. Figure S1: EDS elemental spectrum of 2% Ti-doped ZnO (inset table represents atomic percentages). Figure S2: I-V curve of Au/ZnO/ITO (a) linear scale (b) semi logarithmic scale. Figure S3: Endurance performance of the pure ZnO.

Competing interests

The authors declare that they have no competing interests.

Authors' contributions

AY and DC carried out the sample preparation, participated on its analysis, performed all the analyses, and wrote the paper. SL guided the study and participated in the paper correction. All authors read and approved the final manuscript.

Acknowledgments

The authors would like to acknowledge the financial support from the Australian Research Council Projects of DP110102391, DP1096769, FT100100956 and DP0988687 in this work.

Received: 20 February 2013 Accepted: 22 March 2013

Published: 4 April 2013

References

1. Liu SQ, Wu NJ, Ignatiev A: **Electric-pulse-induced reversible resistance change effect in magnetoresistive films.** *Appl Phys Lett* 2000, **76**(19):2749–2751.
2. Yang JJ, Pickett MD, Li X, Ohlberg DA, Stewart DR, Stanley Williams R: **Memristive switching mechanism for metal/oxide/metal nanodevices.** *Nat Nano* 2008, **3**(7):429–433.
3. Wu SX, Li XY, Xing XJ, Hu P, Yu YP, Li SW: **Resistive dependence of magnetic properties in nonvolatile Ti/Mn: TiO₂/SrTi_{0.993}Nb_{0.007}O₃/Ti memory device.** *Appl Phys Lett* 2009, **94**(25):253504–253506.
4. Beck A, Bednorz JG, Gerber C, Rosse CL, Widmer D: **Reproducible switching effect in thin oxide films for memory applications.** *Appl Phys Lett* 2000, **77**(1):139–141.
5. Chua L: **Memristor—the missing circuit element.** *IEEE Transactions on Circuits Theory* 1971, **18**(5):507–519.
6. Seo JW, Park JW, Lim KS, Yang JH, Kang SJ: **Transparent resistive random access memory and its characteristics for nonvolatile resistive switching.** *Appl Phys Lett* 2008, **93**(22):223505–223507.
7. Strukov DB, Snider GS, Stewart DR, Stanley Williams R: **The missing memristor found.** *Nature* 2008, **453**(7191):80–83.
8. Wang S-y, Tseng T-y: **Interface engineering in resistive switching memories.** *Journal of Advanced Dielectrics* 2011, **1**(2):141–162.
9. Gao B, Zhang HW, Yu S, Sun B, Liu LF, Liu XY, Wang Y, Han RQ, Kang JF, Yu B, Wang YY: **Oxide-Based RRAM: Uniformity Improvement Using A New Material-Oriented Methodology.** Kyoto, Japan: Symposium on VLSI Technology (IEEE); 2009:30–31.
10. Sawa A, Fujii T, Kawasaki M, Tokura Y: **Interface resistance switching at a few nanometer thick perovskite manganite active layers.** *Appl Phys Lett* 2006, **88**:232112–232114.
11. Chang W-Y, Cheng K-J, Tsai J-M, Chen H-J: **Improvement of resistive switching characteristics in TiO₂ thin films with embedded Pt nanocrystals.** *Appl Phys Lett* 2009, **95**:042104–042106.
12. Yoon JH, Kim KM, Lee MH, Kim SK, Kim GH, Song SJ, Seok JY, Hwang CS: **Improvement of resistive switching characteristics in TiO₂ thin films with embedded Pt nanocrystals.** *Appl Phys Lett* 2010, **97**:232904–232906.
13. Guan W, Long S, Jia R, Liu M: **Nonvolatile resistive switching memory utilizing gold nanocrystals embedded in zirconium oxide.** *Appl Phys Lett* 2007, **91**:062111–062113.
14. Chuang WY, Lai YC, Wu TB, Fang SF, Chen F, Tsai M: **Unipolar resistive switching characteristics of ZnO thin films for nonvolatile memory applications.** *J Appl Phys Lett* 2008, **92**:022110–022112.
15. Villafuerte M, Heluani SP, Juarez G, Simonelli G, Braunstein G, Duhalde S: **Electric-pulse-induced reversible resistance in doped zinc oxide thin films.** *Appl Phys Lett* 2007, **90**:052105–052107.
16. Yang YC, Pan F, Liu Q, Liu M, Zeng F: **Fully room-temperature-fabricated nonvolatile resistive memory for ultrafast and high-density memory application.** *Nano Lett* 2009, **9**:1636–1643.
17. Lee S, Kim H, Yun DJ, Rhee SW, Yong K: **Resistive switching characteristics of ZnO thin film grown on stainless steel for flexible nonvolatile memory devices.** *Appl Phys Lett* 2009, **95**:262113–262115.
18. Yang YC, Pan F, Zeng F, Liu M: **Switching mechanism transition induced by annealing treatment in nonvolatile Cu/ZnO/Cu/ZnO/Pt resistive memory: from carrier trapping/detrapping to electrochemical metallization.** *J Appl Phys* 2009, **106**:123705–123709.
19. Kinoshita K, Okutani T, Tanaka H, Hinoki T, Yazawa K, Ohmi K, Kishita S: **Opposite bias polarity dependence of resistive switching in n-type Ga-doped-ZnO and p-type NiO thin films.** *Appl Phys Lett* 2010, **96**:143505–143507.
20. Yao I-C, Lee D-Y, Tseng T-Y, Lin P: **Fabrication and resistive switching characteristics of high compact Ga-doped ZnO nanorod thin film devices.** *Nanotechnology* 2012, **23**:145201–145209.
21. Chung J-L, Chen J-C, Tseng C-J: **Electrical and optical properties of TiO₂-doped ZnO films prepared by radio-frequency magnetron sputtering.** *J Phys Chem Solids* 2008, **69**:535–539.
22. Chung J-L, Chen J-C, Tseng C-J: **The influence of titanium on the properties of zinc oxide films deposited by radio frequency magnetron sputtering.** *Appl Surf Sci* 2008, **254**:2615–2620.
23. Chung J-L, Chen J-C, Tseng C-J: **Preparation of TiO₂-doped ZnO films by radio frequency magnetron sputtering in ambient hydrogen–argon gas.** *Appl Surf Sci* 2008, **255**:2494–2499.
24. Chang H-P, Wang F-H, Chao J-C, Huang C-C, Liu H-W: **Effects of thickness and annealing on the properties of Ti-doped ZnO films by radio frequency magnetron sputtering.** *Curr Appl Phys* 2011, **11**:S185–S190.
25. Lampert A, Mark P: *Current Injection in Solids.* New York: Academic; 1970.
26. Kim JN, Shin KS, Kim DH, Park BO, Kim NK, Cho SH: **Changes in chemical behavior of thin film lead zirconate titanate during Ar⁺-ion bombardment using XPS.** *Appl Surf Sci* 2003, **206**:119–128.
27. Islam MN, Ghosh TB, Chopra KL, Acharya HN: **XPS and X-ray diffraction studies of aluminum-doped zinc oxide transparent conducting films.** *Thin Solid Films* 1996, **280**:20–25.
28. Wagner CD, Riggs WM, Davis LE, Moulder JF, Muilenberg GE: *Handbook of X-ray Photoelectron Spectroscopy.* Eden Prairie, MN: Perkin-Elmer Corporation; 1979:68–69.
29. Studenikin SA, Golego N, Cocivera M: **Carrier mobility and density contributions to photoconductivity transients in polycrystalline ZnO films.** *J Appl Phys* 2000, **87**(5):2413–2422.
30. Henrich VE, Cox PA: *The Surface Science of Metal Oxides.* Cambridge: Cambridge University Press; 1994.
31. Szot K, Speier W, Bihlmayer G, Waser R: **Switching the electrical resistance of individual dislocations in single-crystalline SrTiO₃.** *Nat Mater* 2006, **5**:312–320.
32. Lin CY, Wu CY, Wu CY, Lee TC, Yang FL, Hu C, Tseng TY: **Effect of top electrode material on resistive switching properties of film memory devices.** *IEEE Electron Device Lett* 2007, **28**:366–368.
33. Chu D, Younis A, Li S: *Enhancement of Resistance Switching in Electrodeposited Co-ZnO Films.* ISRN Nanotechnology; 2012:705805.

doi:10.1186/1556-276X-8-154

Cite this article as: Younis et al.: Bi-stable resistive switching characteristics in Ti-doped ZnO thin films. *Nanoscale Research Letters* 2013 **8**:154.